A&A 400, 1065–1070 (2003)
DOI: 10.1051/0004-6361:20030060

Astronomy & Astrophysics

Variation of coronal line widths on and off the disk

E. O'Shea[1], D. Banerjee[2], and S. Poedts[2]

[1] Instituto de Astrofisica de Canarias, C/ vía Láctea s/n, 38200 La Laguna, Tenerife, The Canary Islands, Spain
[2] Centre for Plasma Astrophysics, Katholieke Universiteit Leuven, Celestijnenlaan 200B, 3001 Leuven, Belgium

Received 13 November 2002 / Accepted 15 January 2003

Abstract. We present observations of a Mg x 625 Å coronal line, obtained with the CDS instrument on SoHO, extending from the disk part of the coronal hole to ~90 000 km above the limb in the north polar coronal hole. Observations were performed in polar plumes and inter-plume lanes. To obtain a sufficiently high signal-to-noise ratio the observations were made over long periods of time and subsequent time frames were summed up. For the off-limb observations we notice a turnover point, around 65 000 km above the limb, where the line widths seem to suddenly decrease or level-off. The initial linear increase of line width with altitude supports previous observations and is consistent with an interpretation of linear undamped Alfvèn waves propagating outwards in open field regions. The turnover point seems to indicate the location where a change of physics takes place. We find that this turnover occurs at approximately the same line width value for each of the datasets examined, suggesting that the turnover occurs whenever the non-thermal velocity reaches a certain key velocity. For the on-disk data we find larger widths in the deep coronal hole as compared to the adjacent quiet Sun regions, suggesting the presence of additional waves and/or turbulence in the coronal hole.

Key words. Sun: UV radiation – Sun: atmosphere – Sun: corona

1. Introduction

The measurements of line widths can provide useful information concerning ion temperatures, sub-resolution turbulent motions and velocity fluctuations associated with magnetohydrodynamic waves in the solar corona. Based on SKYLAB data Doschek et al. (1977), Nicolas et al. (1977) and Mariska et al. (1978) have shown that the line width increases with height above the limb. These earlier observations were restricted to temperatures in or below the transition region and thus inferring details concerning coronal heating was not possible. Hassler et al. (1990) obtained line profile data for the coronal Mg x 609/625 Å lines and, although having poor spatial resolution, identified an increase of line width with altitude up to heights of ~70 000 km above the limb, at which point the line width appeared to become constant up to an altitude of 140 000 km. More recently there have been a number of off-limb studies made using the spectrometers onboard SoHO. Doyle et al. (1998) have studied equatorial off-limb line width variations with a Si VIII (~8×10^5 K) line at 1440.49 Å and 1445.75 Å, as observed by SUMER on SoHO. They showed an increase in line width with altitude along with a decrease in density up to 25 000 km above the limb for quiet Sun conditions. Recently Harrison et al. (2002) examined the Mg x 625 Å line (~1×10^6 K) in the equatorial quiet region using the CDS instrument on SoHO. Their most significant result was the discovery of emission line narrowing as a function of altitude and intensity above 50 000 km. All earlier observations of emission line broadening with increasing altitude are consistent with the propagation of linear undamped Alfvén waves in open field regions with decreasing density. Harrison et al. (2002) attributed the narrowing as being due to the dissipation of Alfvèn waves in the corona. One should remember that there is a fundamental difference in the properties of wave propagation in the equatorial corona (closed field regions) as compared to coronal holes (open field regions). Thus it is important to see if one can also observe this narrowing of coronal lines in the coronal hole regions. Both Banerjee et al. (1998) and Doyle et al. (1999) studied Si VIII line profiles with SUMER in the off-limb northern polar hole regions. They recorded line broadening up to 110 000 km (150 arcsec off-limb) and then a levelling off in the line widths up to 220 000 km, after which there was a faint hint of a fall-off in the widths, although this last observation was inconclusive due to uncertainties in the data. Doschek et al. (2001) studied several emission lines (as observed by SUMER), showing increasing width with altitude, again for a coronal hole. Above an altitude of 75 000 km–100 000 km they found a hint of flattening in the width-altitude curves, but the significance of this was in question because of large uncertainties in the data. In the present paper we study the line profiles of a Mg x 625 Å line ($T_e \sim 1 \times 10^6$ K) as observed by CDS on SoHO. The observations were obtained in the disk part of the coronal hole and also in the plumes and inter-plume lanes

Send offprint requests to: E. O'Shea, e-mail: eoshea@ll.iac.es

of the off-limb polar regions. For the disk part we investigate whether there is additional wave activity in the dark coronal hole regions compared to the adjacent quiet Sun regions. For the off-limb polar regions we study the variation of line widths with altitude, up to heights of ~90 000 km above the limb.

2. Observations and data reduction

For these observations we have used the normal incidence spectrometer (NIS) (Harrison et al. 1995), which is one of the components of the Coronal Diagnostic Spectrometer (CDS) on-board the Solar and Heliospheric Observatory (SoHO). The details of the observations including pointing and start times are summarised in Table 1. In order to get good time resolution the rotational compensation was switched off (sit-and-stare mode). The temporal series sequence CHROM_N8 was run and data obtained for 11 transition region and coronal lines formed between 3×10^4 K and 2.5×10^6 K. In this paper, however, we shall only study two of these, the transition region O v 629 Å line ($\sim2.5\times10^5$ K) and the coronal Mg x 625 Å line ($\sim1\times10^6$ K). The data were obtained with the 4×240 arcsec slit with exposure times of 60 s. In order to increase the signal-to-noise ratio we first performed binning by 2 along the slit to produce 70 pixels and then summed in time over the 150 time frames to produce the required line profiles. These line profiles were then fitted with a single Gaussian in order to measure the line widths. Since we are looking at the north polar region the rotation of the Sun should not move our observing region significantly over the duration of the observations despite the fact that we are observing in a sit-and-stare mode.

In Fig. 1 we show the location of the slit for the s23402r00 dataset overlayed on an EIT Fe XII 195 Å image taken at approximately the same time. This figure serves as a representative example for the datasets (28 Sep.–4th October, see Table 1) where we have positioned the centre of the slit roughly at the solar limb so that part of the slit covers the coronal hole region on-disk and part the off-limb region. We also moved the slit in the x-direction once each day to cover the plume regions and the inter-plume lanes, for a comparative study of these two regions off-disk. We have also taken temporal series datasets, with the entire slit almost on the disk (datasets, s23330r00, s23370r00, s23380r00; see Table 1 and Fig. 2) in order to cover part of the quiet Sun and part of the deep coronal hole. This allowed us to perform a comparative study of the coronal hole with the quiet Sun. Details on the CDS reduction procedure may be found in O'Shea et al. (2001). Often scattered light contributions are significant while making observations off-limb. Harrison et al. (2002) have shown in detail that, for the Mg x line, the scattered contribution is very small, so we do not consider any scattered light correction for this analysis.

3. Results

The width of an emission line can be expressed as (McClements et al. 1991),

$$\frac{\Delta\lambda}{\lambda} \propto \left(\frac{kT}{M_i} + \phi + \xi^2\right)^{1/2}, \quad (1)$$

Table 1. A log of the datasets.

Date	Dataset	Pointing (X, Y)	location	Starting time
14/09/01	s23330r00	(−116, 871)	coronal hole	20:23
19/09/01	s23370r00	(59, 865)	coronal hole	16:46
20/09/01	s23380r00	(155, 869)	coronal hole	21:02
28/09/01	s23402r00	(−44, 963)	polar plume	17:21
28/09/01	s23403r00	(−92, 958)	inter-plume	20:27
29/09/01	s23406r00	(4, 960)	inter-plume	17:19
29/09/01	s23407r00	(−199, 935)	polar plume	20:24
30/09/01	s23410r00	(4, 960)	polar plume	12:13
30/09/01	s23411r00	(−40, 961)	inter-plume	15:19
04/10/01	s23451r00	(0, 960)	inter-plume	20:34

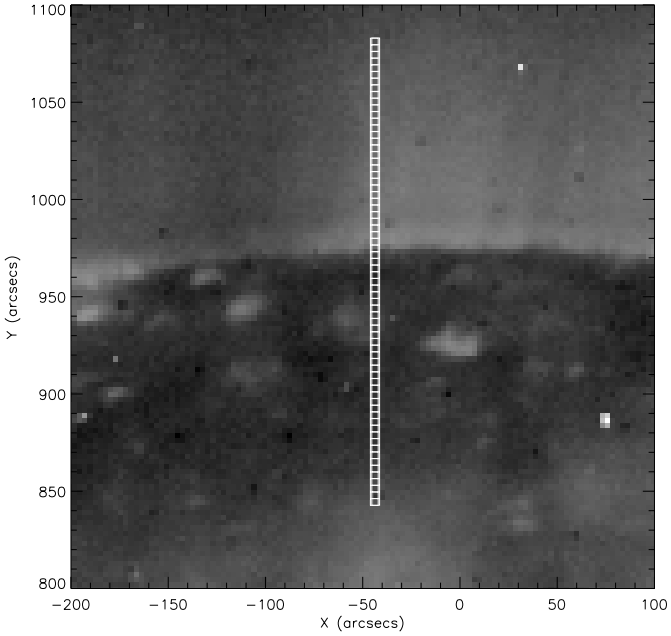

Fig. 1. An Fe XII 195 Å image of the north polar coronal hole taken with EIT on SoHO at 17:24 UT on September 28, 2001. The vertical rectangular box represents the position of the slit corresponding to the s23402r00 dataset. The small squared boxes represent our pixel size.

where the first term on the right hand side represents the natural width of the emission line due to the temperature of the emitting plasma, the second term corresponds to the instrumental width, which is defined by the width of the image of the slit at the detector plane and the third component is due to the non-thermal width i.e. broadening which may be due to turbulence or plasma motions. Implicitly we have assumed that the plasma is in thermal equilibrium, so that the electron and the ion temperatures are the same. For a detailed description of the estimated contributions from the three components for the Mg x 625 Å line please refer to Harrison et al. (2002). In this paper we will always use the 1/e widths. One should also note that the CDS instrument was not designed for line widths studies but, as pointed by Harrison et al. (2002), one can use CDS for

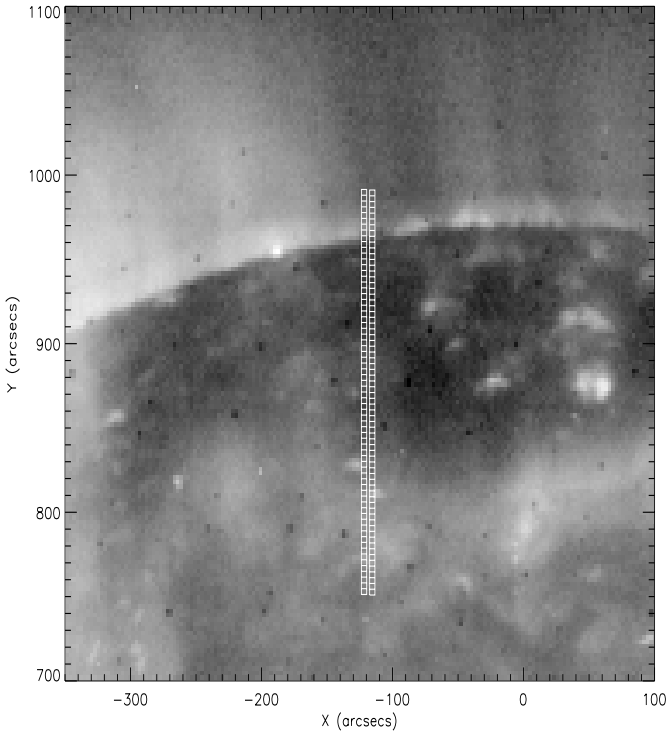

Fig. 2. An Fe XII 195 Å image of the north polar coronal hole taken with EIT on SoHO at 20:26 UT on September 14, 2001. The vertical thin rectangular boxes represent the position of the slit, corresponding to the s23330r00 dataset, at the beginning of the time sequence (right one) and at the end of the time sequence (left one). The small square boxes represent our pixel size.

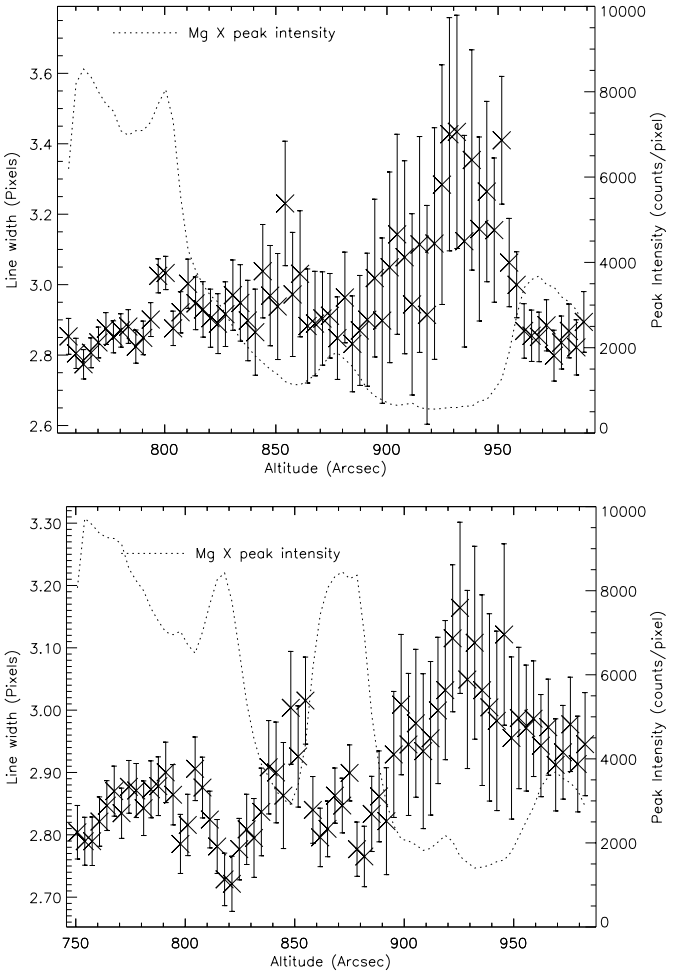

Fig. 3. Variation of the Mg x peak intensity and widths with altitude corresponding to the on-disk data. The upper panel is for dataset s2333000 and the lower panel for dataset s23370r00.

line profile studies provided one has a good line selection and enough statistics.

3.1. On-disk

First we shall present results from the datasets which were taken in such a way that most part of the slit remained on the disk, e.g. Fig. 2. In these datasets the lower part of the slit was positioned on the quiet Sun coronal hole boundary and the upper part on the deep coronal hole, with a small amount of the slit off-limb. In Figs. 3 and 4 we plot the half-width at 1/e intensity, calculated for each Mg x line fit, against its altitude measured in arcsec. The limb is located at around 960 arcsec. In these plots the Mg x intensity variations allow us to identify the coronal hole boundaries as very clearly the lowest intensity regions correspond to the coronal holes. In Fig. 3 (upper panel) the coronal hole is within the 850–950 arcsec range, with the deepest part in the 900–950 arcsec interval. One can clearly see substantial increases in the line widths within that interval. Thus a comparison of the quiet Sun regions, 750–800 arcsec, and the deep coronal hole reveals that there is clear evidence of an increase in non-thermal velocities due to additional plasma motions (e.g. wave activity) and/or turbulence in the coronal hole. This is consistent with the SUMER observations by Hassler et al. (1999) where they found evidence for large outflow velocities in coronal holes. We note that we also found similar results for the s23370r00 dataset where the slit is positioned entirely on the disk (see Fig. 3, lower panel).

Next we shall focus on the disk part of the slit corresponding to the s23402r00 dataset (see Fig. 1 for location). Figure 4 (upper panel) clearly reveals the additional broadening of the Mg x line widths in the darkest locations on the disk, that is, the interval 880–920 arcsec, corresponding to the coronal hole. This is also very evident in Fig. 4 (lower panel) for the s23406r00 dataset where we see a dramatic increase in line width as we move from quiet Sun conditions (840–880 arcsec) to coronal hole conditions (900–940 arcsec).

In the plots shown in Figs. 3 and 4, note that the line widths again decrease as we move from the coronal hole region to the area of the limb, i.e. to altitudes greater than ~950 arcsec. This might be an unexpected result, if we assume that the increase in line widths in the coronal holes is due to propagating waves, as we might have expected the line widths to continue increasing at and above the limb from the values they had in the coronal hole. This fall-off in the line widths at the limb may be due to the fact that at the limb the waves will be predominantly propagating in a direction perpendicular to our line of sight whereas on the disk the waves will propagate in all directions,

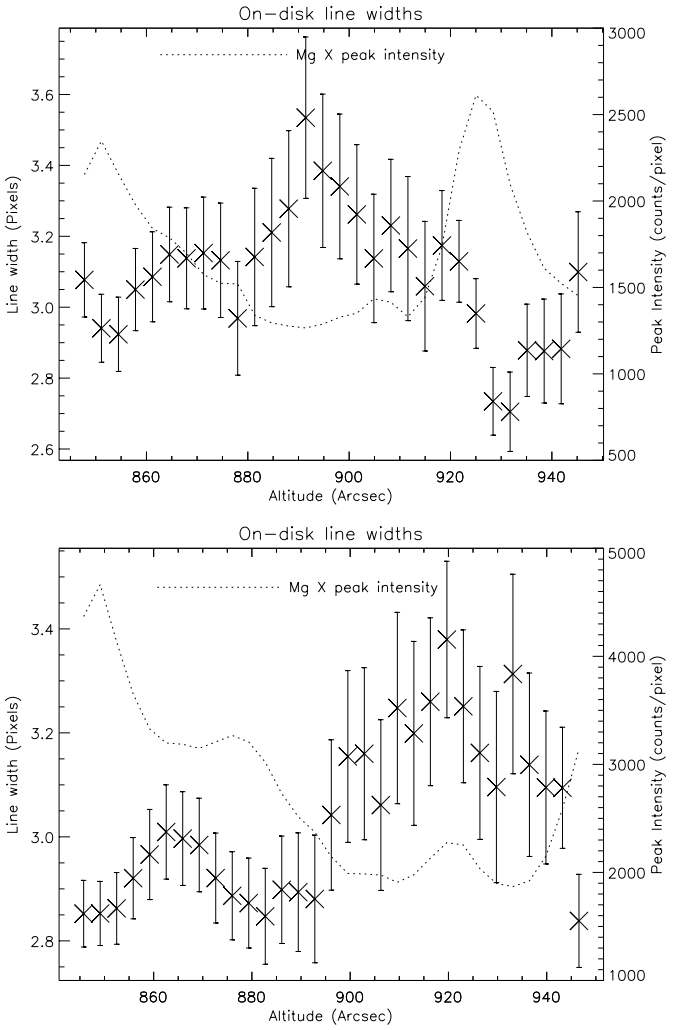

Fig. 4. Variation of the Mg x peak intensity and widths with altitude corresponding to the on-disk data. The upper panel is for dataset s23402r00 and the lower panel for dataset s23406r00.

including those parallel to our line of sight. Hence, near the limb we might expect to see a reduction in the line widths due to the reduced number of waves propagating in our line-of-sight. Similar behavior was noted by Banerjee et al. (2000) in their analysis of SUMER data (see Fig. 5 of Banerjee et al. 2000).

3.2. Off-limb

Now we shall turn our attention to the off-disk datasets. In Fig. 5 we show the variation of the O v peak intensity (dotted line) with altitude for the different datasets. The peak in the intensity curve corresponds to the limb brightening and helps to identify the limb. The measured line widths are shown together with their error bars. For all the datasets we notice a turnover point at a certain altitude where the widths seem to suddenly decrease or level off. To identify this turnover point more accurately we have fitted two linear fits to the measured line widths (solid lines). In Figs. 5a, b we show the results for a plume and inter-plume region respectively for the two datasets of 28 September (s23402r00 and s23403r00). We find in both regions that the line width decreases beyond an altitude of ~1050 arcsec (~62 000 km off-limb). A comparison of Figs. 5a, b also reveals that, in general, the line widths at the same altitude are wider in the inter-plume regions than in the plume. This is consistent with previous results as obtained by SUMER (Hassler et al. 1997; Banerjee et al. 2000). For the 29 September datasets (see Figs. 5c, d) we notice a levelling-off of the widths. We should point out that for the s23407r00 dataset (Fig. 5d) the turnover point appears at lower altitude. The intensity variation of O v reveals that the limb is present at a lower height (around 940 arcsec) than in the other datasets where the limb appears at around 960 arcsec. This is due to the location of the slit ($x = -199$, $y = 935$) in this dataset. In all other datasets the x position is nearer to the disk centre.

Table 2. Details of the turnover points for different datasets.

Date	Dataset	Location (arcsec)	Height (km)	Width (pixel)
28/09/01	s23402r00	1052.85	70 000	3.00
28/09/01	s23403r00	1047.33	65 500	3.03
29/09/01	s23406r00	1052.45	65 600	3.00
29/09/01	s23407r00	1026.46	61 300	2.97
30/09/01	s23410r00	1051.13	64 600	3.00
30/09/01	s23411r00	1049.80	63 500	3.04
04/10/01	s23451r00	1050.62	62 700	2.92

For the 30th September datasets we also notice a turnover point in the line width variation at a certain altitude (Figs. 5e, f). The width appears to be levelling off with not much of an indication of a decrease. We should also mention that for these two datasets the plume and inter-plume variation is not significant as the slit was not positioned very well for such a study. Finally, for the last off-disk dataset, s23451r00 (shown in Fig. 5g), where the slit was positioned along an inter-plume, we also notice a slight fall-off of the widths. Thus, for all the off-limb datasets, we detected a turnover point where the line widths start to decrease or level-off. In Table 2 we summarize the location of these turnover points as observed in all the datasets. It is noticeable that the turnover point occurs almost at the same line width (~3 pixels) in each of the datasets analysed, whether they are in a plume or inter-plume region. This suggests that the turnover occurs whenever the non-thermal velocity reaches a certain key velocity. Unfortunately with the CDS instrument it is not possible to measure non-thermal velocity estimates due to large uncertainties in the instrumental width (see Harrison et al. 2002).

4. Conclusion

For the on-disk observations we find an excess in the line widths in the regions corresponding to the coronal holes, in comparison with the adjacent quiet Sun regions, indicating the presence of an additional non-thermal velocity component in the coronal holes. This additional non-thermal component suggests the presence of plasma motions, probably in the form of propagating waves, and/or turbulence, which is consistent with SUMER results, as presented by Hassler et al. (1999), of outflow

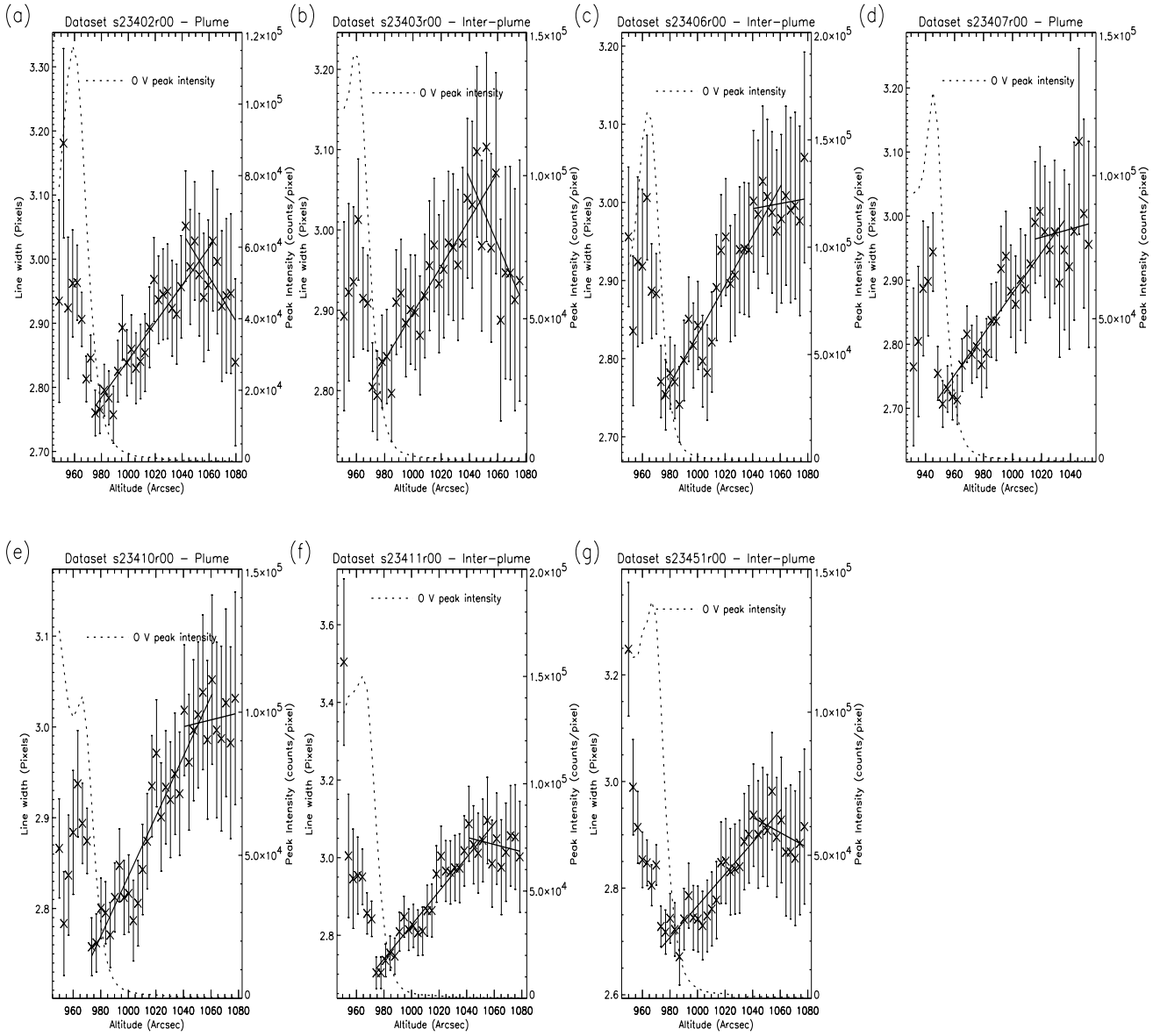

Fig. 5. Variation of the Mg x line width (half 1/e width) with altitude corresponding to the different datasets as labelled. The dotted lines in each plot show the variation of the O v intensity with altitude which is useful for identifying the solar limb. The solid lines correspond to the best-line fit to the observed line widths.

velocities in coronal holes. As we go outside the limb we observe that at certain heights the line widths are wider in the inter-plume lanes as compared to the plumes, signifying that the inter-plume lanes seem to be preferred for wave propagation and the acceleration of the fast solar wind. This result also confirms published SUMER results, e.g. Hassler et al. (1997); Banerjee et al. (2000). The most significant result of the present analysis is the identification of the turnover point.

It is well known that the Alfvén waves propagate virtually undamped through the quasi-static corona and deposit their energy flux in the higher corona. For the coronal holes with open magnetic field configuration the energy flux density due to Alfvén waves can be written as (Doyle et al. 1998),

$$F = \sqrt{\frac{\rho}{4\pi}} < \delta v^2 > B\,, \qquad (2)$$

where ρ is the plasma mass density, $< \delta v^2 >$ the mean square velocity, which is related to the observed non-thermal velocity as $\xi^2 = \frac{1}{2} < \delta v^2 >$, where the factor of 2 accounts for the polarization and direction of propagation of a wave relative to the line of sight, and B, is the magnetic field strength. Thus, for a constant value of F propagating in the regions of decreasing density and magnetic field, the value of ξ must increase. This can explain the almost linear increase of width with altitude for all previous studies and also for the current observations in the low part of the corona (roughly within the range 960–1050 arcsec in our work). Beyond this point (we call it the turnover point ~65 000–70 000 km above the limb) the levelling off or falling off can not be explained with simple expressions like Eq. (2). It is possible that the linear theory of adiabatic wave propagation breaks down beyond this point or some form of dissipation (e.g. phase mixing) becomes

important. We note that this turnover or levelling off in the line widths occurs at approximately the same line width value (~3 pixels) in each of the datasets examined, suggesting that the turnover occurs whenever the non-thermal velocity reaches a certain key velocity. Torkelsson et al. (1998) have studied numerically the propagation of non-linear spherical Alfvén waves in a radial magnetic field. They show that the wave damps by forming current sheets in which the Poynting flux is lost to Ohmic heating and the acceleration of upflow. We hope that our observational results provide constraints on the modelling of the acceleration of the fast solar wind. Finally, we should point out that the present observations were limited to certain heights above the limb. If we go further out we should be able to see a clearer picture of line width narrowing. We hope to pursue this in a forthcoming campaign.

Acknowledgements. DB wishes to thank the FWO for a fellowship (G.0344.98). EOS is a member of the European PLATON Network (`http://www-solar.mcs.st-and.ac.uk/~thomas/platon`). We would like to thank the CDS and EIT teams at Goddard Space Flight Center for their help in obtaining the present data. CDS and EIT are part of SoHO, the Solar and Heliospheric Observatory, which is a mission of international cooperation between ESA and NASA.

References

Banerjee, D., Teriaca, L., Doyle, J. G., & Wilhelm, K. 1998, A&A, 339, 208
Banerjee, D., Teriaca, L., Doyle, J. G., & Lemaire, P. 2000, Sol. Phys., 194, 43
Doschek, G. A., Feldman, U., & Cohen, L. 1977, ApJS, 33, 10
Doschek, G. A., Feldman, U., Laming, J. M., Schühle, U., & Wilhelm, K. 2001, ApJ, 546, 559
Doyle, J. G., Banerjee, D., & Perez, M. E. 1998, Sol. Phys., 181, 91
Doyle, J. G., Teriaca, L., & Banerjee, D. 1999, A&A, 349, 956
Harrison, R. A., Sawyer, E. C., Carter, M. K., et al. 1995, Sol. Phys., 162, 233
Harrison, R. A., Hood, A. W., & Pike, C. D. 2002, A&A, 392, 319
Hassler, D. M., Rottman, G. J., Shoub, E. C., & Holzer, T. E. 1990, ApJ, 348, L77
Hassler, D. M., Wilhelm, K., Lemaire, P., & Schühle, U. 1997, Sol. Phys., 175, 375
Hassler, D. M., Dammasch, I. E., Lemaire, P., et al. 1999, Science, 283, 810
McClements, K. G., Harrison, R. A., & Alexander, D. 1991, Sol. Phys., 131, 41
Mariska, J. T., Feldman, U., & Doschek, G. A. 1978, ApJ, 226, 698
Nicolas, K. R., Brueckner, G. E., Tousey, R., et al. 1977, Sol. Phys., 55, 305
O'Shea, E., Banerjee, D., Doyle, J. G., Fleck, B., & Murtagh, F. 2001, A&A, 368, 1095
Torkelsson, Ulf., & Boynton, G. C. 1998, MNRAS, 295, 55